

IDENTIFYING 14 MHZ PROPAGATION MODES USING FST4W SNR AND SPECTRAL SPREAD

Gwyn Griffiths G3ZIL

gwyn@autonomousanalytics.com

Abstract

The FST4W protocol within the WSJT-X family of weak signal communications programs has an advantage over the widely used WSPR protocol in that it estimates spectral spreading. With modern equipment of modest cost, readily available to the radio amateur, spectral spread at the transmitter and receiver can be less than 30 mHz. This is much lower than spectral spread imposed on signals by ionospheric refraction or ground or sea scatter. Simple two-dimensional scatter plots of spectral spread and signal to noise ratio, alongside time series plots, show clear clustering attributable to different propagation modes. Using a single FST4W transmitter in Northern California and reports from eleven receivers from 2.4 km to over 3000 km to the west, north and east spectral spreading/signal to noise ratio clusters for surface wave and ionospheric 1F and 2F paths were easily identifiable. Other clusters were not so obvious. In particular, the prevalence of 2F ground side-scatter, or skew off great circle propagation, also termed 'above the basic maximum usable frequency' propagation, at ranges of 40 to 1000 km was unexpected. This mode was also seen after dusk at more distant receivers, following on from 1F propagation as the maximum usable frequency fell. This mode was easily tracked across different receivers by its high spectral spread, 500 mHz to 650 mHz, some eight times that of 1F propagation. Instances of 'above the basic maximum usable frequency' nighttime propagation due to, we hypothesize, refraction from patches in the ionosphere with much higher electron density than the background plasma were identified by their low spectral spreading at 1000 km and 1525 km. Identifying the particular propagation mode over a path may be of interest to the radio amateur, for example, if the current mode is 2F ground side-scatter, antenna headings along the great circle path may not give best results. Propagation mode identification using FST4W could be a radio amateur contribution to the ionospheric science programs of the 2023 and 2024 Festivals of Eclipse Science, charting changes in propagation modes as changes in solar flux affected ionospheric dynamics and structure.

1. Motivation

The original motivation for this study was to try and identify the propagation mechanism for horizontally polarized transmissions on 14 MHz from WB7ABP, Santa Rosa, Ca. received at KPH, Point Reyes, Ca., a distance of about 40 km. The question arose during an investigation into WSPR spots decoded from signals scattered by passenger aircraft involving WB7ABP transmissions and KPH reception. Conventional wisdom has it that the horizontally polarized ground wave signals from WB7ABP, received on the horizontally polarized TCI530 antenna at KPH could not have produced the +7 dB SNR in 2.5 kHz that was observed with little variation over 24 hours.

The study expanded beyond the 40 km path from WB7ABP to KPH in order to:

- (a) Investigate whether the mechanism was also present on other paths.
- (b) Include paths where, with certainty, the mechanism was magneto-ionic refraction in the ionosphere F layer.
- (c) Assess whether the two-parameter method adopted for this study - SNR and spectral spreading from using the FST4W mode within the WSJT-X package - could identify other propagation mechanisms.

This report is structured as follows: Section 2 describes the December 2022 experiment, the data collection and analysis methods and summarises candidate propagation mechanisms, Section 3 shows the results for each path with an analysis and synthesis in Section 4, and a discussion and thoughts for future work in section 5.

2. The December 2022 Experiment

The main experiment ran from 1600 UTC 29 December 2022 to 0800 UTC 31 December 2022 with additional periods at WW6D and from 1600 UTC 3 January 2023 to 1800 UTC January 2023 to see if a surface wave path was possible inland to KP4MD.

Transmitter: The single transmitter was an ANAN-100D at WB7ABP, Santa Rosa, Ca. (CM88ok, Calif., 38.44°N 122.79°W) with 5 W output to a 5-element horizontally polarized KT-34XA Yagi beam¹ directed northwest, with a beamwidth of about 50°. The mode was FST4W-120 with a 1 in 3 duty cycle. A phase-locked GPSDO master oscillator ensured frequency stability and low spectral spreading. The location is shown as the red map pin in Figure 2.1.



Figure 2.1. Map of the transmitter (red) at WB7ABP and receiver (yellow) locations for the December 2022 experiment. Map courtesy Google Earth.

Receivers: All receivers whose data were used in this experiment were KiwiSDRs running WsprDaemon, release v3.0.5 or later except for an Elad receiver with WJT-X 2.5.4 at WW6D. Their locations are the yellow map pins in Figure 2.1. Spots from the local receiver WB7ABP/K are shown for completeness and to show no outages in transmissions. These receivers were running KiwiSDR firmware version 1.557 or later ensuring that the spectral spreading contribution, if using the out-of-the-box GPS aiding, was of order 50 mHz. Some sites used a phase-locked GPSDO with their KiwiSDR (N6GN/K, WA2TP). We chose not to use the phase-locked receiver at KFS to show that

¹ See <https://www.hammanuals.com/MMans/KT-34XA.pdf>

the results and subsequent interpretation could be done elsewhere with a standard KiwiSDR or equivalent.

The paths: Despite the constraint of requiring receivers set up for FST4W and, with one exception, report data to the WsprDaemon extended spots database to gather spectral spreading data automatically, a rich set of contrasting paths was possible:

- Local group - 0 to 150 km - covering near field (WB7ABP/K), ground (or surface) wave (WW6D), 40 km SSW to a coastal site (KPH), 121 km SSE to a coastal site including over seawater (KFS), 133 km NE inland (KP4MD).
- 500 – 1525 km, all over land, comprising 645 km ESE (ND7M), 679 km N (KK6PR), and 960 km NE (KA7OEI-1) and 1525 km ENE (N6GN/K),
- 4210 km, transcontinental, over land, ENE (WA2TP).
- 3762 km seawater path except for ~30 km, WSW (AI6VN/KH6).
- Into the auroral oval, 3392 km N (INUVIK).

Geomagnetic conditions: During the experiment the geomagnetic conditions, Table 2.1, spanned quiet to disturbed, certainly not 'very quiet' with M class solar flares on two days. The smoothed December 2022 sunspot number was taken as 103 for use in propagation and ray trace modelling.

Date	Mid Lat A	Max flare	time UTC	SSN	Solar flux	Kp max
29 Dec	8	M2	1833	88	160	3
30 Dec	22	M3	1938	113	163	5
31 Dec	10	C9	2148	121	162	3.3

Table 2.1 Indicators of geomagnetic and solar conditions for 29-31 December 2022. The A index is for Fredericksburg, Kp is the planetary maximum for the day, SSN is sunspot number and solar flux is the standard flux at 10.7 cm. Data from <https://www.swpc.noaa.gov/> and <https://spaceweather.com/>.

FST4W - estimation of SNR and spectral spread: Details of the FST4W's estimation of spectral spread are available² in Griffiths et al. (2022). Unpublished work has shown that while interference from co-channel WSPR signals can affect FST4W SNR and spectral spread the WSPR SNR has to be at least 8dB above that of the FST4W signal, and overlapping, to produce statistically significant outliers. Using median values in this study avoids possible errors from co-channel interference.

Data collection: The KiwiSDRs used Rob Robinett's WsprDaemon software version 3.0.3 or later³ to report data, including FST4W spectral spreading, to the WsprDaemon extended spots database⁴. The single exception was for WW6D where screen capture text files from WSJT-X FST4W, where an empty file *specplot* was added to the directory from where WSJT-X was run, were manually imported into the WsprDaemon database. WW6D's location provided the only short-distance (2.4 km) line of sight path for assured ground wave reception.

3. Results

The results for each path are shown as time series of:

- SNR in dB in a bandwidth of 2.5 kHz superimposed with altitude of the sun at the mid point of a great circle path. The geographical location of receivers was calculated⁵ from their grid

² TAPR/ARRL Digital Communications Conference Proceedings at https://files.tapr.org/meetings/DCC_2022/2022%20DCC1.pdf

³ <https://github.com/rrobinett/wsprdaemon>

⁴ See <http://wsprdaemon.org/> for details of WsprDaemon including guides on how to access the database.

⁵ <https://www.giangrandi.org/electronics/radio/qthloccalc.shtml>

location and the great circle bearing, distance and mid point obtained using an online calculator⁶. The mid points were set as variables for each path in the Grafana dashboard, to be used with the Sun and Moon data source plugin from C. Fetzer⁷.

- FST4W spectral spread in mHz.
- Noise level in dBm in 1 Hz bandwidth at the antenna socket of the KiwiSDR estimated using the FFT method using the total power in the lowest power 30% of spectral estimates within the 200 Hz band⁸. At sites with low local noise the record can show periods when propagated-in noise dominated or was absent.
- Signal level in dBm calculated from the SNR and the noise level, referenced to the antenna input socket of the KiwiSDR, unfortunately not a free space estimate that would allow comparison between sites. Nevertheless this can be a useful parameter as the effect of co-variation of signal and noise levels can be removed.

On each SNR time series panel one or more periods are given labels:

- N - near field, only for WB7ABP/K at the transmitter site.
- G - ground wave, at WW6D, distance 2.4 km.
- A - uncertain propagation mode, only applicable at KPH and, very briefly, at KFS, with relatively high SNR and low spectral spread; split into A1 and A2 at KPH to show day-to-day variation.
- B - uncertain propagation mode, applicable in the Local Group to 150 km range, higher SNR than label A but high spectral spread.
- C - only observed at KFS, lower SNR than label B with medium spectral spread.
- I - assessed as various forms of ionospheric propagation modes; split into I1-I7 where there were distinct patterns to the SNR and spectral spread.

For each path a scatterplot of spectral spread and SNR is annotated with the identifying label from the time series together with summary statistics. The statistics are: median and median absolute deviation for SNR and spectral spreading, median-based robust statistics being more appropriate for these parameters, and the standard deviation of the frequency.

⁶ <https://www.movable-type.co.uk/scripts/latlong.html>

⁷ <https://fetzerch.github.io/2016/07/03/grafana-sunandmoon-datasource/> installed from the zip file.

⁸ Griffiths, G., Robinett, R. and Elmore, G. 2020. Estimating LF-HF band noise while acquiring WSPR spots. *QEX*, ARRL, Sept-Oct 2020.

3.1 WB7ABP self-decode



Figure 3.1. Time series of SNR with sun elevation, spectral spread, noise level and signal level for WB7ABP at same location reporting as WB7ABP/K.

Near field path: Single mode

Propagation Mode: Near field. The near field reception provides assurance over the presence of transmissions but does not produce reliable quantitative information on SNR or spectral spread because of severe overload of the KiwiSDR.

(Figure 3.2 has been deleted).

3.2 WB7ABP to WW6D 2.4 km ground wave line-of-sight except for suburban structures

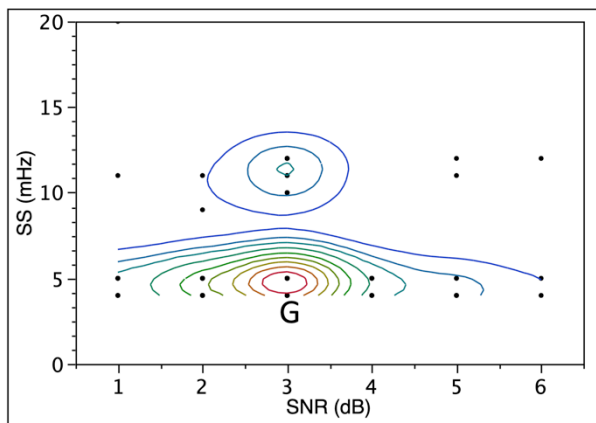


Figure 3.3. Time series of SNR with sun elevation, spectral spread, noise level and signal level for WB7ABP at WW6D. This record does not have signal level as it was obtained using WSJT-X version 2.5.4 hence no noise level or signal level.



Figure 3.4. Elevation profile from WB7ABP (left) to WW6D (right). Note that with antenna heights of 50' at WB7ABP and 30' at WW6D this is a line of sight path except for suburban structures. Courtesy Google Earth.

2.4 km path - single mode



Label G: Ground wave: very low SS.
 Median (SNR)= 3.0dB MAD (SNR)= 0.8 dB
 median (SS)=5.0 mHz MAD (SS)=2.7 mHz

Figure 3.5. Scatterplot with density contours of single cluster spectral spread and SNR at WW6D.

3.3 WB7ABP to KPH 40 km SSW to a coastal receiver



Figure 3.6. Time series of SNR with sun elevation, spectral spread, noise level and signal level for WB7ABP at KPH.



Figure 3.7. Elevation profile from WB7ABP (left) to KPH (right). Courtesy Google Earth.

40 km path - two modes

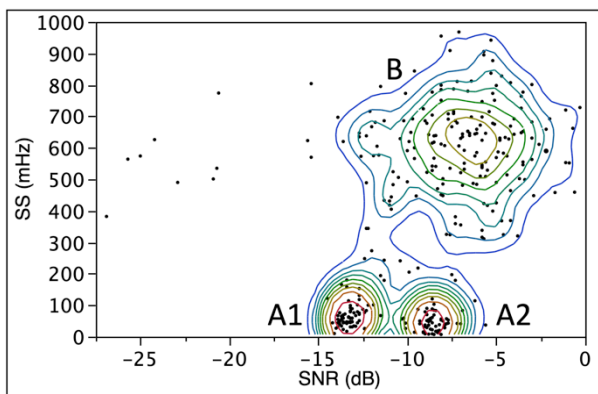


Figure 3.8. Scatterplot with density contours of spectral spread and SNR showing distinct separation of the two clusters labelled A (A1 and A2 on the two days) and B at KPH.

Label A: Lower SNR and much lower SS (by factor 10), essentially nighttime complementary to mode B. SNR distributions have different medians on the two days.

Median (SNR)= -11.3 dB MAD (SNR)=2.3 dB
 median (SS)=59 mHz MAD (SS)=27 mHz SD (freq)=0.05 Hz

Label B: Higher SNR, high SS and frequency variation, essentially daytime, starting just after sunrise and persisting until just after sunset.

Label B is not always present each day in a longer time series than shown

Median (SNR)= -6.8 dB MAD (SNR)=1.8 dB
 median (SS)=624 mHz MAD (SS)=83 mHz SD (freq)=0.46 Hz

3.4 WB7ABP to KFS 121 km SSE to a coastal receiver



Figure 3.9. Time series of SNR with sun elevation, spectral spread, noise level and signal level for WB7ABP at KFS.



Figure 3.10. Elevation profile from WB7ABP (left) to KFS (right), the flat path is over seawater of San Francisco Bay. Courtesy Google Earth.

121 km path - three modes

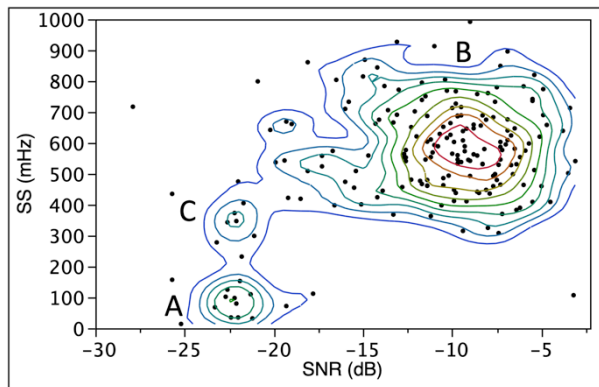


Figure 3.11. Scatterplot with density contours of spectral spread and SNR showing distinct separation of three labelled clusters A, B and C at KFS.

Label A: Lower SNR and lower SS, essentially nighttime, complementary to cluster label B. One spot only 30 Dec at 0404 UTC, and 13 between 0240 and 0404 UTC on 31 Dec.

Median (SNR)= -22.2 dB MAD (SNR)=0.7 dB median (SS)=118 mHz MAD (SS)=48 mHz SD (freq)=0.05 Hz

Label B: Higher SNR, high SS and frequency variation, essentially daytime, starting just after sunrise and persisting until just after sunset.

Median (SNR)= -9.7 dB MAD (SNR)=2.4 dB median (SS)=580 mHz MAD (SS)=99 mHz SD (freq)=0.43 Hz

Label C: Lower SNR and medium SS, nighttime after label B, possibly two spots this label on 30 Dec, 10 on 31 Dec. Median (SNR)= -21.9 dB MAD (SNR)=0.5 dB median (SS)=288 mHz MAD (SS)=154 mHz SD (freq)=0 Hz.

3.5 WB7ABP to KP4MD 133 km NE inland



Figure 3.12. Time series of SNR with sun elevation, spectral spread, noise level and signal level for WB7ABP at KP4MD.



Figure 3.13. Elevation profile from WB7ABP (left) to KP4MD (right). Courtesy Google Earth.

133 km path - one mode

Label B: Higher SNR, high SS and frequency variation, essentially daytime, starting after sunrise and persisting until just after sunset.

Median (SNR)= -19.1 dB MAD (SNR)=2.4 dB
 media n(SS)=585 mHz MAD (SS)=97 mHz SD (freq)=0.35 Hz.

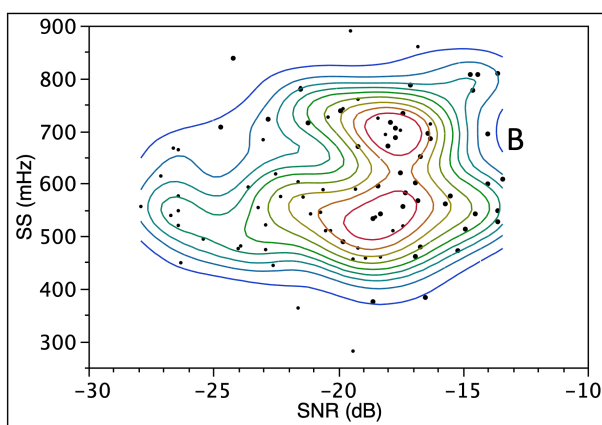


Figure 3.14. Scatterplot with density contours of spectral spread and SNR showing the single cluster with label B at KP4MD, with two peaks due to day-to-day variability.

3.6 WB7ABP to ND7M 645 km to inland Nevada



Figure 3.15. Time series of SNR with sun elevation, spectral spread, noise level and signal level for WB7ABP at ND7M.

645 km path - two modes

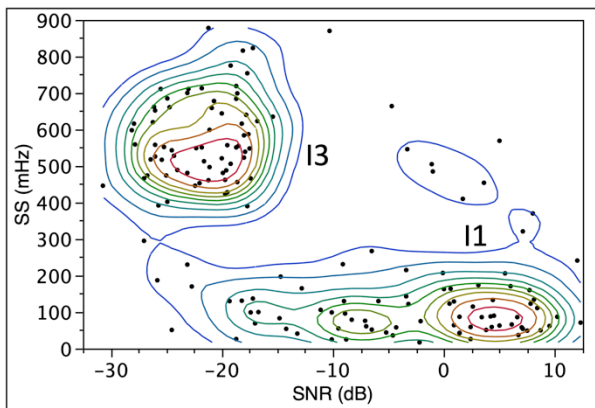


Figure 3.16. Scatterplot with density contours of spectral spread and SNR showing distinct separation of two labelled clusters I1 and I3 at ND7M.

Label I1: High SNR, with low SS, essentially daytime, continuous on 29/30 Dec, but interspersed with I3 on 30/31 Dec, with some instances at night.

Median (SNR)= 1.4 dB MAD (SNR)=5.7 dB
 median (SS)=88 mHz MAD (SS)=39 mHz SD (freq)=0.32 Hz.

Label I3: Low SNR, high SS, daytime and past sunset at mid point but also interspersed with I1 on 30/31 Dec.

Median (SNR)= -22.3 dB MAD (SNR)=3.6 dB
 median (SS)=549 mHz MAD (SS)=67 mHz SD (freq)=0.33 Hz.

3.7 WB7ABP to KK6PR 679 km inland to Oregon



Figure 3.17. Time series of SNR with sun elevation, spectral spread, noise level and signal level for WB7ABP at KK6PR.

679 km path - two modes

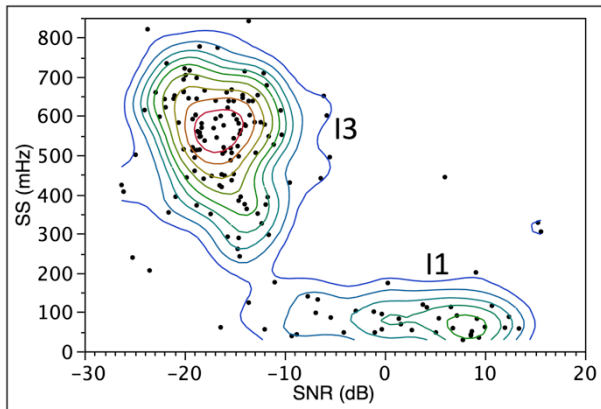


Figure 3.18. Scatterplot with density contours of spectral spread and SNR showing distinct separation of two labelled clusters I1 and I3 at KK6PR.

Label I1: High SNR, with low SS, almost continuous on 29/30 Dec, but interspersed with I3 on 30/31 Dec.

Median (SNR)= 3.8 dB MAD (SNR)=4.9 dB
 median (SS)=69 mHz MAD (SS)=21 mHz SD (freq)=0.37 Hz.

Label I3: Low SNR, high SS, daytime and past sunset at mid point but also interspersed with I1 on 30/31 Dec.

Median (SNR)= -16.9 dB MAD (SNR)=2.7 dB
 median (SS)=578 mHz MAD (SS)=62 mHz SD (freq)=0.27 Hz.

3.8 WB7ABP to KA7OEI-1 960 km inland to Northern Utah



Figure 3.19. Time series of SNR with sun elevation, spectral spread, noise level and signal level for WB7ABP at KA7OEI-1 (Northern Utah SDR site).

960 km path - three modes

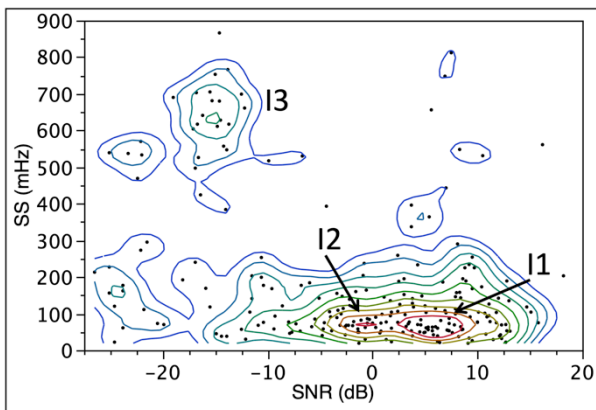


Figure 3.20. Scatterplot with density contours of spectral spread and SNR showing modest separation of two labelled clusters I1 and I2 at KA7OEI-1 but a clear separation from cluster I3.

Label I1: High SNR, but variable, with low SS, essentially daytime.

Median (SNR)= 5.4 dB MAD (SNR)=3.7 dB
 median (SS)=87 mHz MAD (SS)=38 mHz SD (freq)=0.35 Hz.

Label I2: Lower SNR, but still with low SS, nighttime.

Median (SNR)= -3.4 dB MAD (SNR)=7.2 dB
 median (SS)=77 mHz MAD (SS)=28 mHz SD (freq)=0.11 Hz.

Label I3: Low SNR, but steady and decreasing with time, high SS, nighttime, before clusters labelled I2 were I3 present.

Median (SNR)= -15.2 dB MAD (SNR)=1.3 dB
 median (SS)=623 mHz MAD (SS)=76 mHz SD (freq)=0.41 Hz.

3.9 WB7ABP to N6GN/K 1525 km inland to Colorado



Figure 3.21. Time series of SNR with sun elevation, spectral spread, noise level and signal level for WB7ABP at N6GN/K.

1525 km path - three modes

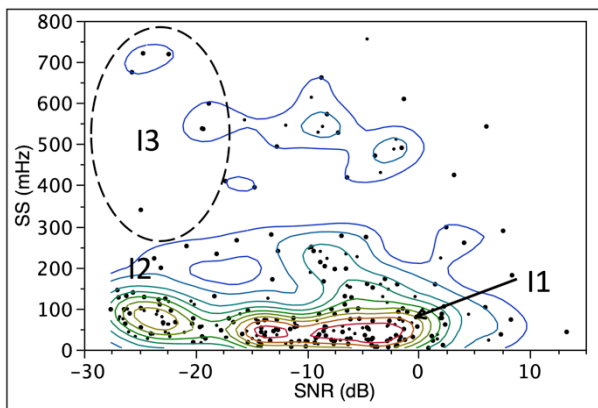


Figure 3.22. Scatterplot with density contours of spectral spread and SNR showing distinct separation of three labelled clusters I1, I2 and I3 at N6GN/K.

Label I1: High SNR, but variable, with low SS, essentially daytime.

Median (SNR)= -6.2 dB MAD (SNR)=3.5 dB
 median (SS)=67 mHz MAD (SS)=55 mHz SD (freq)=0.24 Hz.

Label I2: Lower SNR, but still with low SS, nighttime.

Median (SNR)= -20.2 dB MAD (SNR)=4.7 dB
 median (SS)=73 mHz MAD (SS)=30 mHz SD (freq)=0.13 Hz.

Label I3: Lower SNR and high SS, nighttime.

Median (SNR)= -19.4 dB MAD (SNR)=3.1 dB
 median (SS)=538 mHz MAD (SS)=160 mHz SD (freq)=0.51 Hz.

3.10 WB7ABP to WA2TP 4210 km transcontinental to New York



Figure 3.23. Time series of SNR with sun elevation, spectral spread, noise level and signal level for WB7ABP at WA2TP.

4210 km path - one mode

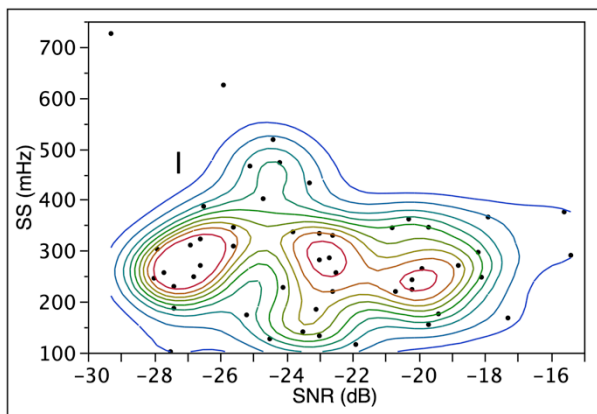


Figure 3.24. Scatterplot with density contours of spectral spread and SNR showing a single cluster with variations in SNR during daily openings at WA2TP.

Label I: Before and after dusk at midpoint.
 Median (SNR)= -23.2 dB MAD (SNR)=3.0 dB
 median (SS)=277 mHz MAD (SS)= 65mHz
 SD (freq)=0.42 Hz.

3.11 WB7ABP to AI6VN/KH6 3762 km to Maui, all but 30 km over seawater



Figure 3.25. Time series of SNR with sun elevation, spectral spread, noise level and signal level for WB7ABP at AI6VN/KH6.

3762 km path - two modes

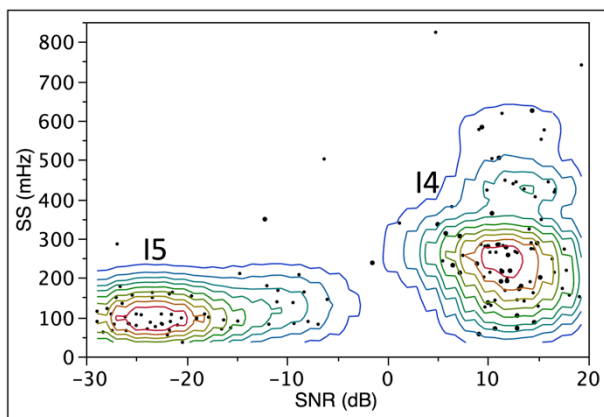


Figure 3.26. Scatterplot with density contours of spectral spread and SNR showing distinct separation of two labelled clusters I4 and I5 at AI6VN/KH6.

Label I4: High SNR, with medium SS, daytime.

Median (SNR)= 11.9 dB MAD (SNR)=2.3 dB
 median (SS)=266 mHz MAD (SS)=83 mHz
 SD (freq)=0.46 Hz.

Label I5: Lower SNR, lower SS, nighttime, starting some hours after sunset at mid point.

Median (SNR)= -21.7 dB MAD (SNR)=4.2 dB
 median (SS)=83 mHz MAD (SS)=20 mHz SD (freq)=0.09 Hz.

3.12 WB7ABP to INUVIK 3392 km N overland to 68°N, Northern Territory, Canada



Figure 3.27. Time series of SNR with sun elevation, spectral spread, noise level and signal level for WB7ABP at INUVIK.

3392 km path - two modes

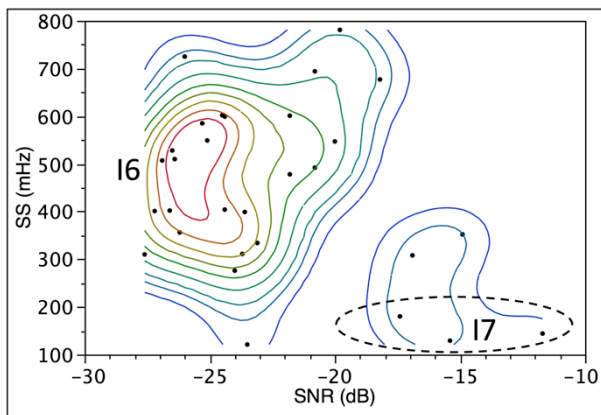


Figure 3.28. Scatterplot with density contours of spectral spread and SNR showing two labelled clusters I6 and I7 at INUVIK. The automatic contouring included spots with higher spectral spread than the true I7 cluster that has been manually determined within the dotted contour.

Label I6: Low SNR, high SS, spanning sunset at mid point.

Median (SNR)= -24.2 dB MAD (SNR)=2.4 dB
 median (SS)=500 mHz MAD (SS)=101 mHz
 SD (freq)=0.46 Hz.

Label I7: Higher SNR, lower SS, as path closes.

Median (SNR)= -16.4 dB MAD (SNR)=2.9 dB
 median (SS)=137 mHz MAD (SS)=12 mHz
 SD (freq)=0.36 Hz.

4. Synthesis

In this section we attempt to ascribe the SNR and SS clusters identified for each receiver in Section 3 to particular propagation modes. In several cases we have compared received SNR time series to predicted SNR from a point-to-point prediction model. The model chosen is Proppy⁹, an online version of the ITU's ITURHFPROP application based on Recommendation ITU-R P.533-14¹⁰ implemented by James Watson (M0DNS). Proppy includes WSPR as a traffic option for SNR calculation, whose properties are close enough to FST4W-120 for the purposes of this study. In an admitted oversimplification, justified by the exploratory nature of this study, the transmit and receive antennas are set as dipoles at 20 m. Consequently, any match in SNR levels is fortuitous, the main features looked for in the comparisons with predictions are timings of openings.

4.1 500 – 1525 km over land

Label I1: Considering first the 960 km to KA7OEI-1, Figure 4.1 shows the path and predicted SNR as a function of time UTC and frequency. The red line is the Operational MUF as defined in ITU-R P373-9¹¹ and is 1.1 to 1.35 times the basic MUF that is based on the critical frequency for the ordinary wave for the F2 layer (f_oF_2). Extracting the predicted SNR for 14 MHz and plotting alongside the observed SNR and spectral spreading gives the time series in Figure 4.2.

The alignment of mode I1 with the prediction based on f_oF_2 suggests strongly that the mode identified as I1, with high SNR and low spectral spreading, corresponds to single-hop magneto-ionic refraction in the F2 layer.

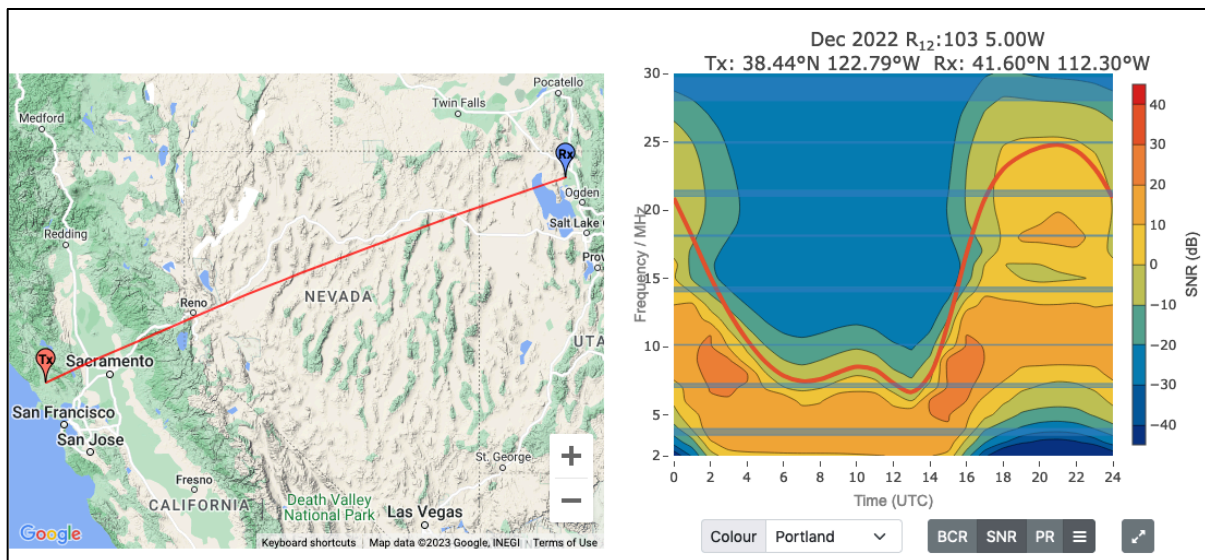


Figure 4.1 From Proppy: Map of the path from WB7ABP to KA7OEI-1 together with the 24-hour SNR prediction with frequency chart for December 2022.

⁹ <https://soundbytes.asia/propy/p2p>

¹⁰ https://www.itu.int/dms_pubrec/itu-r/rec/p/R-REC-P.533-14-201908-I!!PDF-E.pdf

¹¹ https://www.itu.int/dms_pubrec/itu-r/rec/p/R-REC-P.373-9-201309-I!!PDF-E.pdf

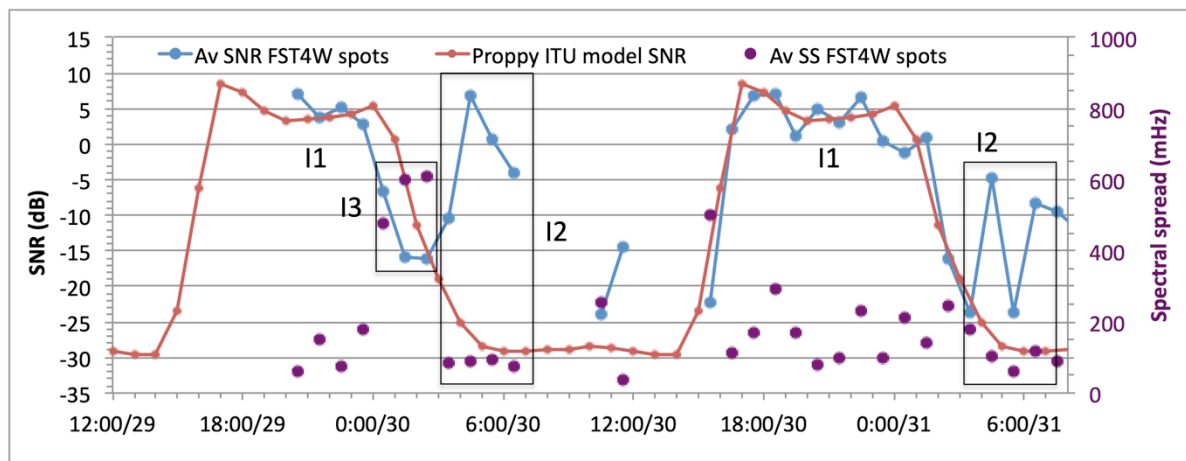


Figure 4.2 Time series of observed SNR at KA7OEI-1 (blue) with the repeated SNR prediction of Proppy (red) assuming rural noise and FST4W spectral spread (purple). The shape and dynamic range of the main daily SNR peak is consistent between the observations and Proppy, but Proppy does not show the nighttime peak.

Label I2: For this path I2 is observed during the night, with a median SNR of about 9 dB below the daytime F2 level and a low spectral spreading, median 28 mHz. Examination of contemporaneous ionosonde profiles at the Idaho National Laboratory (600 km NE of the path mid point, 195 km N of KA7OEI-1) showed that I2 was an example of above-the-MUF propagation. McNamara et al. (2008)¹². Their paper looked at two mechanisms: normal magneto-ionic refraction from "quasi-random elemental patches of ionization" with higher electron density than the background plasma (also referred to as 'ionospheric roughness') and two-hop ground side-scatter, that is, off the great circle path and to the receiver, such that each hop is supported by the MUF at the time. The following is a working hypothesis for I2.

I2 arose from one-hop F layer propagation via magneto-ionic refraction from patches of higher ionization, given the following observations / assumptions:

- I2 showed low spectral spreading, which, as a working assumption, we associate with magneto ionic refraction rather than ground side scatter which we assume would show greater spectral spread.
- The drop in SNR is modest, at 9 dB, which would tend to rule out the ever-present ionospheric scattering mode that would likely have a much lower SNR, and, reinforcing this view, I2 is not ever-present.

Label I3: There is no equivalent in the propagation prediction to I3, present only on 30 December at KA7OEI-1. The following set out two hypotheses for Label I3, the first based only on the record at KA7OEI-1, and the second also considering records at ND7M (645 km) and KK6PR (679 km).

- A. I3 arose from two-hop E layer propagation, given the following observations / assumptions:
- I3 was present between 0028 UTC and 0258 UTC on 30 December and not at all on 31 December - it is an intermittent mode.
 - The closest ionosonde record, at the Idaho National Laboratory, showed a strong blanketing E layer between 0400 UTC and 0645 UTC, peaking at 0515 UTC with an foEs of 6.1 MHz¹³. The duration is similar to that of the I3 event, but displaced in time by 3.5 hours - it is known that 'clouds' of E layer activity drift.

¹² McNamara, L.F., Bullett, T.W., Mishin, E. and Yampolski, Y.M., 2008. Nighttime above-the-MUF HF propagation on a midlatitude circuit. *Radio Science*, 43(2).

¹³ Select 30 December at

<https://lgdc.uml.edu/common/DIDBDayListForYearMonthAndStation?ursiCode=IF843&year=2022&month=12>

- Mid-latitude one-hop magneto-ionic refraction from the F2 layer, as in mode I1, is associated with low spectral spread. While we have yet to obtain FST4W records from unequivocal E layer propagation the working assumption here is that single hop E layer propagation would not induce 16 times the observed spectral spreading of F2 mode I1. Barnum (1968)¹⁴ however, found that ground forward-scatter reflections from irregularities caused "severe vertical broadening" of oblique ionosonde records. Thus our assumption of a two-hop E layer propagation with intermediate ground forward scatter.
- B. I3 arose from an above the basic MUF (ABM) mechanism such as ground side-scatter over a 2F two-hop path, not along the great circle, but of an unknown geometry where each hop was supported by the MUF at the time, as discussed in McNamara et al. (2008) and summarised in ITU report ITU-R P.2011:
- I3 was present throughout the day and past sunset on 29/30 Dec 2022 at ND7M (645 km ESE to 0252 UTC, section 3.6) and KK6PR (679 km N to 0258 UTC, section 3.7). The persistence through daylight hours and presence in orthogonal directions some 650 km apart argue against propagation via two-hop sporadic blanketing E layer, hypothesis A.
 - The intermediate ground side-scatter provides the mechanism for the observed high spectral spreading (some eight times that of 1F refraction) and the much lower SNR over 1F refraction.
 - The Recommendation ITU-R P.533 model (section 6.2 in 15) has a simple model for the excess loss L_m above the loss where the operating frequency f is at, or lower than, the basic MUF fb for path distance D . For $D < 7000$ km and F layer propagation, when $f > fb$:

$$L_m = 36 \left[\frac{f}{fb} - 1 \right]^{1/2} \text{ dB or } 62 \text{ dB whichever is the smaller.}$$

fb was calculated for 1830 UTC 29 December 2022 to 0330 UTC 30 December 2022 for paths of 645 km and 679 km corresponding to receivers at ND7M and KK6PR and mode I3 identified in Figures 3.15 and 3.17 by extrapolation for the ionosonde MUFs at 600 km and 800 km from the Idaho National Lab. Table 4.1 gives the median excess loss L_m calculated from the above equation for $f = 14.097$ MHz over the period when fb was over 8 MHz, avoiding the time of rapid fall-off in the evening, and the observed median excess loss over the mode I1 SNR.

Receiver	Path length (km)	Median L_m model (dB)	Median L_m meas (dB)
ND7M	645	22.7	26.6
KK6PR	679	22.1	22.4

Table 4.1 Model and observed excess loss L_m for paths to ND7M and KK6PR.

The agreement at KK6PR is (quite frankly) astonishing, given that the mode I1 SNR was measured the following day, that antenna response may be different between the mode 1 great circle path and off great circle ground side-scatter two hop paths. The agreement is not as good at ND7M, but the difference of 4 dB is not substantial, and it is in the expected direction, that is, greater L_m at the shorter distance (lower fb).

¹⁴ Barnum, J.R., 1968. *Mixed-Mode Oblique Ionograms: A Computer Ray-Tracing Interpretation*. Stanford University Ca., Stanford Electronics Labs., available at <https://apps.dtic.mil/sti/pdfs/AD0845620.pdf>

The balance of evidence favours 2F (that is, two-hop) ABM propagation over sporadic 2E for mode I3 in the records at ND7M, KK6PR and KA7OEI-, and, intermittently, as the band closed on 30 December 2023 at N6GN/K, Figure 3.21. This is because 2F ABM explains the propagation during daylight hours at ND7M and KK6PR as well as the post sunset period on the 960 km path to KA7OEI-1 as the MUF fell, and the two even briefer periods on the 1525 km path to N6GN/K also as the MUF fell.

4.2 4210 km transcontinental path over land

Label I: is, with high certainty, 2F magneto-ionic refraction. Despite the ~25 dB discrepancy in SNR between the Proppy prediction and the observed average hourly values in Figure 4.3 the timing of the openings is consistent between model and observations. Analysis using PyLap confirmed the two-hop 2F hypothesis, one-hop along 070° from WB7ABP only reaching to 2000 km at the December SSN of 103 (at the minimum elevation angle of 2°). The 2F determination reinforces our hypothesis that ground scatter leads to spectral spread

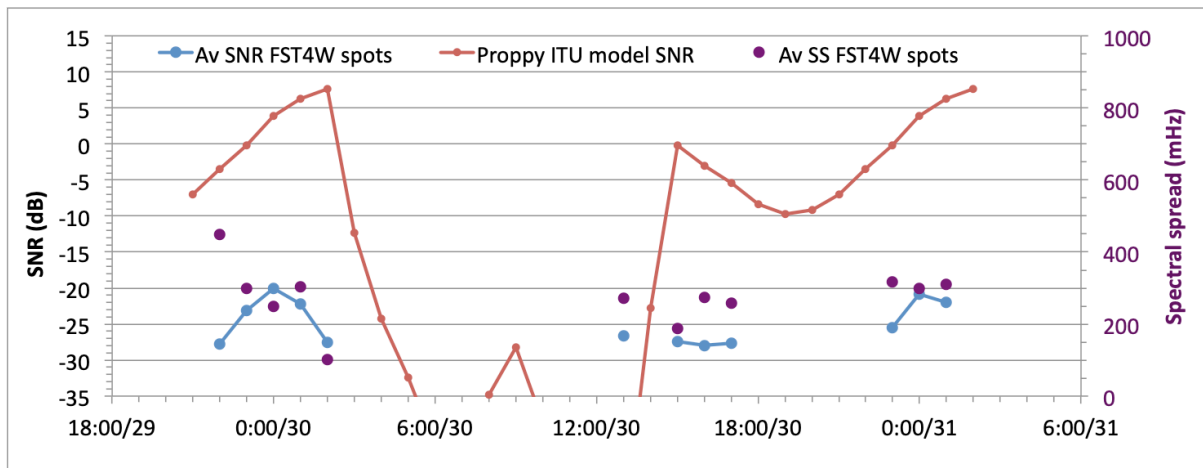
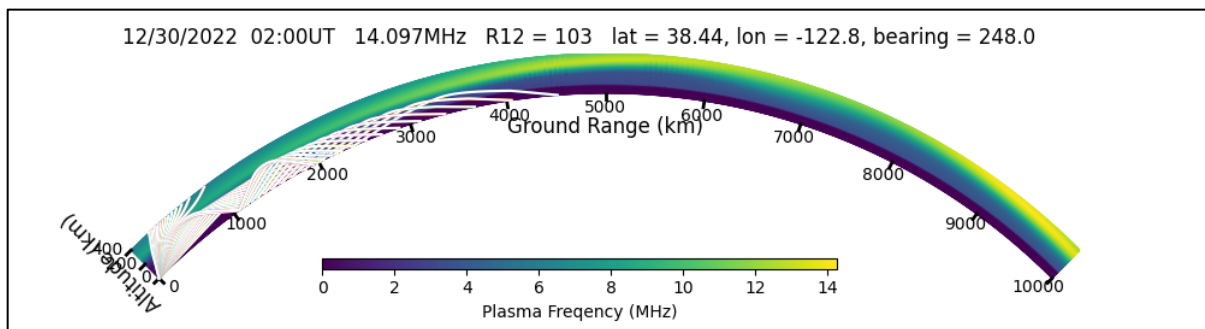


Figure 4.3 Time series of observed SNR at WA2TP (blue) with the repeated SNR prediction of Proppy (red) assuming residential noise and FST4W spectral spread (purple). While there is no agreement on the absolute SNR the observed spots did occur at the peaks of the model prediction.

4.3 3762 km seawater path to AI6VN/KH6

Label I4: is, with high certainty, 2F magneto-ionic refraction from PyLap ray tracing, Figure 4.4 top. The median spectral spreading, at 266 mHz, was essentially the same as the 277 mHz on the 2F 4210 km overland path to WA2TP.

Label I5: is very likely to be 1F magneto-ionic refraction, where the 83 mHz median spectral spread was very similar to the 1F paths to N6GN/K (73 mHz) and KA7OEI-1 (87 mHz). While a PyLap ray tracing at 0645 UTC does show 1F to ~3300 km, Figure 4.4 bottom, the 1F path in the simulation is short-lived (tens of minutes) not the four hours observed on 30 December 2022 and, at 2° elevation, did not quite reach 3762 km. In this instance 1F propagation lasts significantly longer than in the PyLap model.



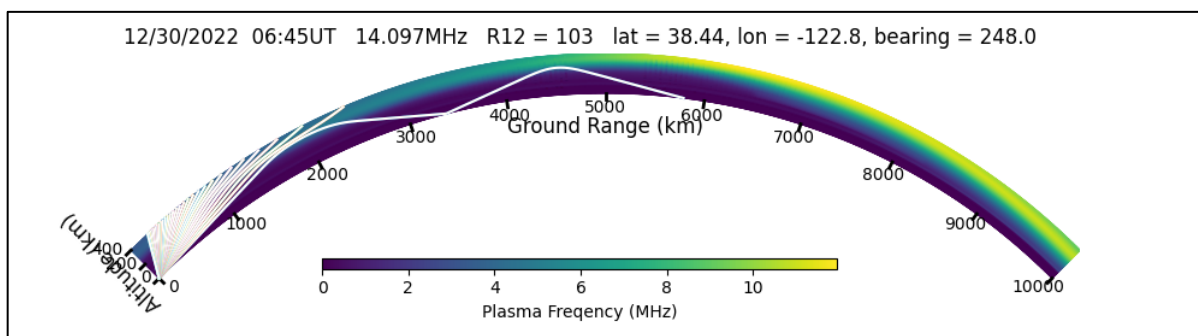


Figure 4.4 Top: PyLap ray traces showing two-hop propagation from WB7ABP to AI6VN/KH6 at 3762 km on a bearing of 248° during the high SNR period identified as I4 in Figure 3.25. Bottom: PyLap showed that short-lived one-hop propagation to over 3000 km was possible around the time the band closed. The observations in Figure 3.25, particularly the low spectral spread, suggested that the one-hop mode persisted for some four hours.

4.4 3392 km into the auroral oval to Inuvik

Labels I6 and I7: Inuvik, Northwest Territory, Canada at 68.35°N is mostly either within the Auroral Oval, or to the north. Figure 4.5 shows the predicted position of the Auroral Oval for 15 January 2023 when Kp was 3, which was the situation for much of the experiment in December 2022. The blue circle shows the estimated position of the refraction by the ionosphere of the second hop of the 2F propagation path, assumed to be one quarter of the total path distance from Inuvik. Being within the Auroral Oval was a factor in the 2F spectral spread on this path (500 mHz) being almost double that on mid-latitude 2F paths of similar distance (277 mHz to WA2TP and 266 mHz to AI6VN/KH6). We would expect the spectral spreading to be even greater under geomagnetic disturbed or storm conditions, with reduced decode probability². With little doubt, we attribute I6 to 2F propagation.

The four out of thirty spots that were assessed as 1F would have been refracted by the ionosphere some 850 km to the south, away from the Auroral Oval, however the 1F spectral spreading on this path (137 mHz) was, nevertheless, substantially higher than on mid-latitude paths (e.g. 73 mHz to N6GN/K, 83 mHz to AI6VN/KH6). On this evidence, we attribute I7 to 1F propagation, backed up with the PyLap ray trace in Figure 4.6.

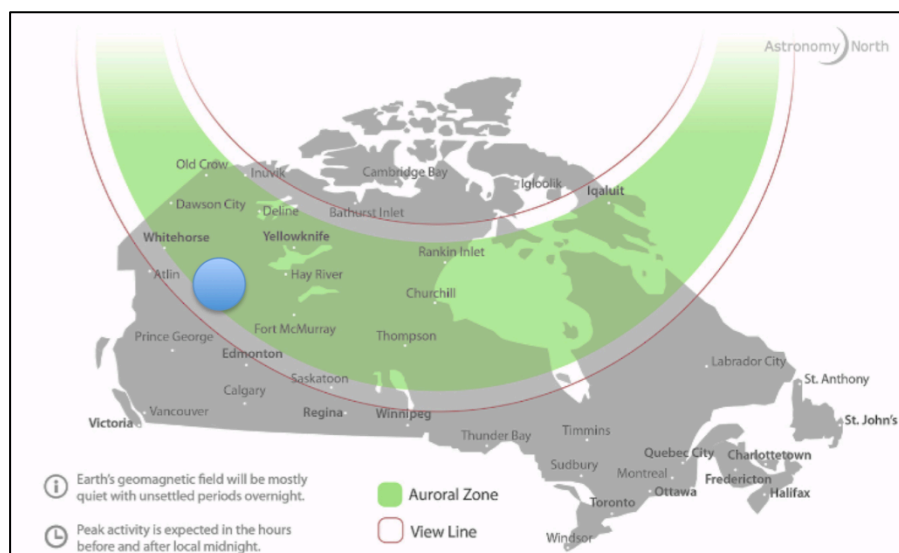


Figure 4.5. Map of the predicted position and extent of the Auroral Oval in green for Kp=3 on 15 January 2023 from <https://astronomynorth.com> together with an estimate of the zone for the second hop refraction from the ionosphere for 2F propagation.

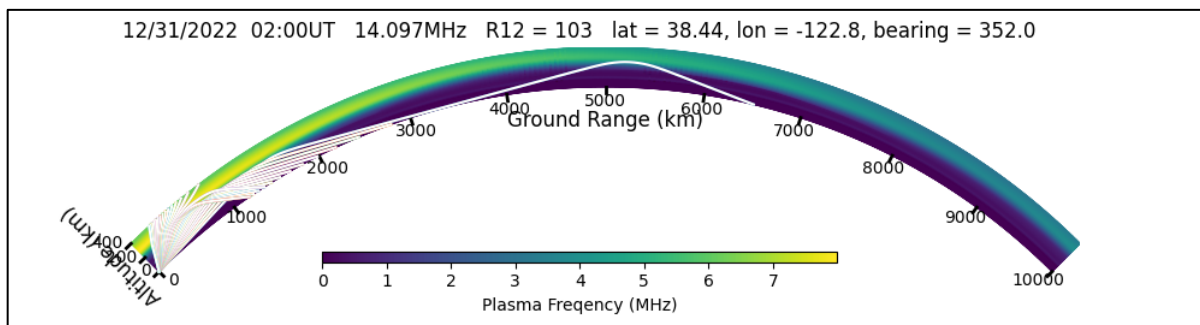


Figure 4.6 Top: PyLap ray traces showing one-hop propagation from WB7ABP to LNUVIK at 3392 km on a bearing of 352° during the low spectral spread period identified as I7 in Figure 3.27.

4.5 The Local Group

The original motivation for this study was to identify the modes with labels A, B and C in this local group.

Label B: Our approach of first attributing SNR/spectral spreading clusters to specific propagation modes for distances of over 600 km has proved useful. Figure 4.7 plots the median spectral spreading together with end points at plus and minus the standard error of the median where we have identified the mode as 2F ABM. The median spectral spreading for the clusters labelled B in the Local Group are within the range for the more distant receivers. Therefore, our working hypothesis is that B in the Local Group represents 2F ABM propagation. Unfortunately, we do not have instances of 1F propagation at these shorter distances against which to calculate the SNR reduction for 2F ABM.

Label A: Our working assumption is that A represents ground (or surface wave) propagation based on the following:

- Rare (10 out of 177 spots) and with low SNR at KFS, distance 121 km, and not present at all at KP4MD at 133 km at a site with residential rather than rural noise level.
- Present 47% of the time at KPH, distance 40 km, as a lower SNR, lower spectral spread nighttime mode after the MUF had dropped sufficiently low for the SNR from 2F ABM propagation to drop below that of the ground wave; the ground wave being weak as horizontally polarized antennas were in use at each end.

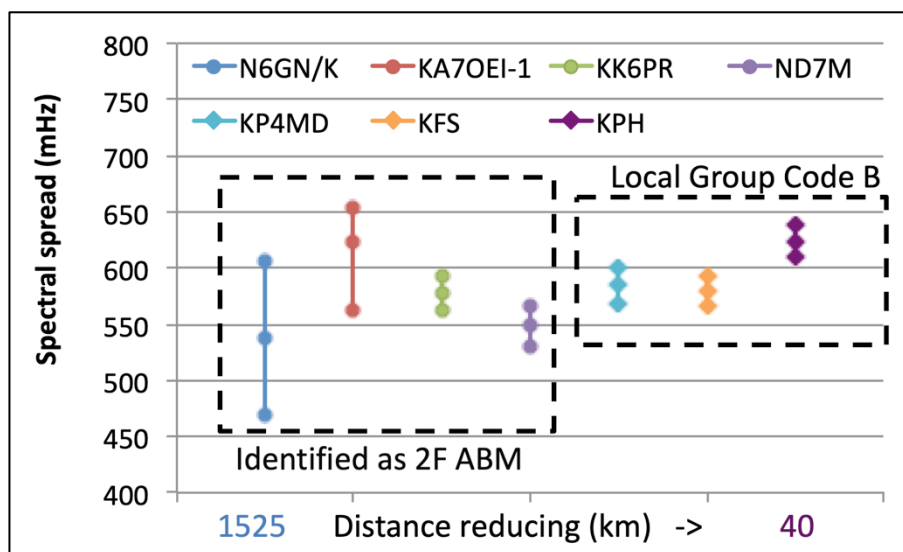


Figure 4.7. Median spectral spread with the end-points at plus and minus one standard error of the median for the four receivers where the mode was identified as 2F ABM propagation together with the medians for label B in the Local Group, the implication being that label B propagation mode was 2F ABM.

Label C: We do not have a credible hypothesis for this mode. These are the relevant facts:

- KFS was the only station where this mode was received.
- Moreover, it was only received on two of the station's four antennas¹⁵:
 - On Omni_A, an omnidirectional TCI530-5-02 log periodic antenna with a nominal gain of 6 dBi, as reported in section 3.4, and on the SE sector antenna, a TCI527B "*super high gain log-periodic*" with a nominal gain of 15 dBi, a front-to-back ratio of 13 dB, and a beamwidth of 64° centred on 135°. The label C median SNR was -21.9 dB on Omni_A (11 spots) and -24.1 dB on the SE antenna (15 spots).
 - The mode was not received on the NW sector antenna, a TCI532-4-02 log periodic with a nominal 12 dBi gain directed 278°, or the SW sector antenna of the same type directed toward 222°.
- This mode was not present every day, but label A, ascribed to ground wave, was also not present to the same extent every day.
- The median spectral spreading at 288 MHz on Omni_A was seen on 2F paths from the summary in section 4.6, but 2F is not a credible hypothesis for a nighttime mode over a 121 km path.

Our conjecture is that the spots in cluster C were from multipath ground wave, perhaps involving diffraction and or scattering, perhaps involving the northern Santa Cruz mountains that form the spine of San Francisco peninsula inland from KFS at Half Moon Bay, and occurred only under circumstances we have yet to determine or understand.

4.6 Summary of assignment to propagation modes

Table 4.2 summarises the assignment of the initial SNR/spectral spreading cluster labels to recognised modes of propagation determined or hypothesised in the preceding sections, with label C being the only cluster without a credible hypothesis.

¹⁵ Antenna details are at <https://www.klofas.com/blog/2021/picoballoon-launch-11/KFS-KiwiSDR.pdf>

Path	Dist (km)	Initial Label	Mode	med SNR (dB)	mad SNR (dB)	med SS (mHz)	mad SS (mHz)
WW6D	2.4	G	Gnd wave	3.0	0.8	5.0	2.7
KPH	40	A	Gnd wave	-11.3	2.3	59	27
		B	2F ABM	-6.8	1.8	624	83
KFS	121	A	Gnd wave	-22.2	0.7	118	48
		B	2F ABM	-9.7	2.4	580	99
		C	Unknown	-21.9	0.5	288	154
KP4MD	133	B	2F ABM	-19.1	2.4	585	97
ND7M	645	I1	1F	1.4	5.7	88	39
		I3	2F ABM	-22.3	3.6	549	67
KK6PR	679	I1	1F	3.8	4.9	69	21
		I3	2F ABM	-16.9	2.7	578	62
KA7OEI-1	960	I1	1F	5.4	3.7	87	38
		I2	1F IR	-3.4	7.2	77	28
		I3	2F ABM	-15.2	1.3	623	76
N6GN/K	1525	I1	1F	-6.2	3.5	67	55
		I2	1F IR	-20.2	4.7	73	30
		I3	2F ABM	-19.4	3.1	538	160
WA2TP	4210	I	2F	-23.2	3.0	277	65
AI6VN/KH6	3762	I4	2F	11.9	2.3	266	83
		I5	1F	-21.7	4.2	83	20
INUVIK	3392	I6	2F	-24.2	2.4	500	101
		I7	1F	-16.4	2.9	137	12

Table 4.2. Summary of the attribution to propagation modes for the SNR/spectral spreading clusters observed at the eleven receivers in this study. IR is Ionospheric Roughness, and ABM is Above the Basic MUF - taken to be ground side-scatter. the propagation mode for the cluster identified with label C at KFS remains unknown.

5. Discussion

If only SNR was available, for example from WSPR, it would have been far more difficult to assign the received spots to propagation mode with any degree of confidence. SNR alone is so dependent on local conditions at the receiver, making it difficult to compare SNR values across sites. It is the combination of the spectral spreading measurement from FST4W and the frequency stability of the WB7ABP transmitter and KiwiSDR and ELAD receivers, together with SNR, that has made the assignment to propagation mode possible.

Most of the paths showed more than one propagation mode, at times alternating over tens of minutes, but more often the propagation modes followed in succession on a daily cycle as the MUF changed. The degree of separation of the SNR/spectral spreading clusters was surprising, most showing no ambiguity at all between clusters. This was either because the change of propagation mode was fast, with few intermediate spots, or else there was a clear gap in time between the instances of the distinct modes. Recognising the spectral spreading associated with a mode on a clear and unambiguous path made it easier to spot the same mode on a path where, beforehand, there had been no explanation for the propagation mode. This was especially true for the 2F ground side-scatter mode on paths from 40 km to 1525 km. Indeed, experienced radio amateurs did not, before this study, immediately associate this mode with propagation at 14 MHz over these paths.

The method described could prove useful for determining propagation modes on paths across continental North America before, during and after the 14 October 2023 annular eclipse and the 8 April 2024 total solar eclipses as changes in solar flux impact ionosphere dynamics and structure.

The cluster with label C, only observed occasionally on two of the antennas at KFS, a path of 121 km, remains a mystery. It is possible that longer time series, making full use of the directionality from

the four antennas, and systematically altering the heading of the transmit Yagi antenna may lead to a better characterisation and subsequently to an attribution for this mode.

Acknowledgement

The author is grateful to Lynn Rhymes WB7ABP for providing the precise frequency FST4W transmissions and to the following for providing FST4W spots: Doug Bender (WW6D), the Maritime Radio Historical Society (KPH); Craig McCartney W6DRZ, Globe Wireless Radio Services and KFS Radio Club (KFS); Carol Milazzo (KP4MD), Dennis Benischek (ND7M), Rick Wahl (KK6PR), Clint Turner (KA7OEI), Glenn Elmore (N6GN), Rob Robinett (AI6VN), Bryan Klofas (KF6ZEO for Inuvik), and Tom Paratore (WA2TP). This study could not have been performed without the WsprDaemon software package from Rob Robinett and FST4W by the WSJT-X development team.